Figure S5

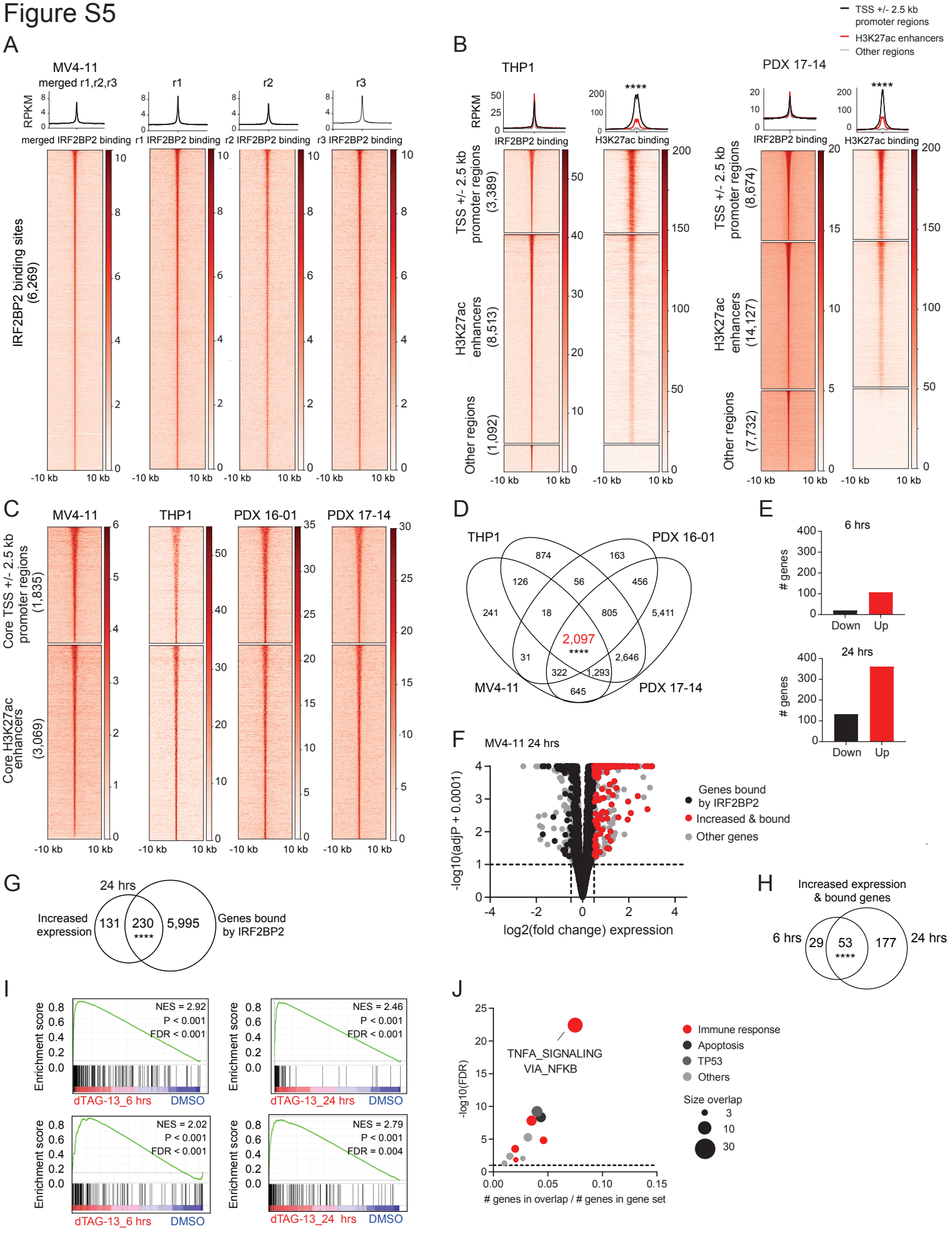
A
MV4-11
merged r1,r2,r3
r1
r2
r3
RPKM
merged IRF2BP2 binding
r1 IRF2BP2 binding
r2 IRF2BP2 binding
r3 IRF2BP2 binding
IRF2BP2 binding sites (6,269)
-10 kb
10 kb
B
TSS +/- 2.5 kb promoter regions
H3K27ac enhancers
Other regions
THP1
PDX 17-14
IRF2BP2 binding
H3K27ac binding
****
TSS +/- 2.5 kb promoter regions (3,389)
H3K27ac enhancers (8,513)
Other regions (1,092)
TSS +/- 2.5 kb promoter regions (8,674)
H3K27ac enhancers (14,127)
Other regions (7,732)
C
MV4-11
THP1
PDX 16-01
PDX 17-14
Core TSS +/- 2.5 kb promoter regions (1,835)
Core H3K27ac enhancers (3,069)
D
THP1
PDX 16-01
MV4-11
PDX 17-14
874
163
126
56
456
241
18
805
5,411
2,097
****
31
2,646
322
1,293
645
E
6 hrs
24 hrs
genes
Down
Up
F
MV4-11 24 hrs
-log10(adjP + 0.0001)
log2(fold change) expression
Genes bound by IRF2BP2
Increased & bound
Other genes
G
24 hrs
Increased expression
131
230
****
5,995
Genes bound by IRF2BP2
H
Increased expression & bound genes
6 hrs
29
53
****
177
24 hrs
I
Enrichment score
NES = 2.92
P < 0.001
FDR < 0.001
dTAG-13_6 hrs
DMSO
NES = 2.46
P < 0.001
FDR < 0.001
dTAG-13_24 hrs
DMSO
NES = 2.02
P < 0.001
FDR < 0.001
dTAG-13_6 hrs
DMSO
NES = 2.79
P < 0.001
FDR = 0.004
dTAG-13_24 hrs
DMSO
J
-log10(FDR)
TNFA_SIGNALING VIA_NFKB
genes in overlap / # genes in gene set
Immune response
Apoptosis
TP53
Others
Size overlap
3
10
30

Figure S5. IRF2BP2 acts as a transcriptional repressor in AML

A, Heatmaps and read density metaplots of IRF2BP2 signal on IRF2BP2 genome-wide binding sites +/-10 kb in MV4-11 cells. Three ChIP-seq replicates (r1, r2, and r3) generated using three different IRF2BP2 antibodies were merged into a single IRF2BP2 ChIP-seq sample (IRF2BP2 merged r1, r2, r3). Shown is the IRF2BP2 RPKM normalized signal for the merged data and for each individual replicate r1, r2, r3, ranked by the IRF2BP2 merged binding signal.

B, Clustered heatmaps and metaplots showing genome-wide IRF2BP2 chromatin binding +/- 10kb regions in THP1 (left) and PDX 17-14 cells (right). Heatmaps showing area under the curve RPKM normalized signal for IRF2BP2 and H3K27ac binding. The IRF2BP2 binding sites were grouped into three clusters based on the promotor/ enhancer status: promotor regions (TSS +/- 2.5kb), enhancers, and other regions, depicting peaks not classified as promotors or enhancers. Clustered regions were ranked by IRF2BP2 signal. Read density metaplots are showing average RPKM normalized signal for IRF2BP2 and H3K27ac in promotor regions (black), H3K27ac enhancers (red) and other regions (gray). Differential read density in promotor versus H3K27ac enhancer regions was evaluated by unpaired t-test with Welch's correction, **** $p < 0.0001$.

C, Clustered heatmaps and metaplots showing from the left to right IRF2BP2 chromatin binding +/- 10kb on the core (common) regions in MV4-11, THP1, PDX 16-01 and PDX 17-14 cells. The IRF2BP2 binding sites were grouped into two clusters based on the promoter/enhancer status: promoter regions (TSS +/- 2.5 kb) and enhancers. Clustered core regions were ranked by IRF2BP2 signal in MV4-11 cells.

D, Venn diagram depicting the overlap of the IRF2BP2 nearest target genes in MV4-11, THP1, PDX 16-01 and THP1 cells. Highlighted red is the number of IRF2BP2 core (common) target genes.

E, Barplots showing the number genes with increased expression (red) and decreased expression (black) post degradation of IRF2BP2 at 6 hours (upper panel) and at 24 hours (lower panel) in MV4-11 cells.

F, Volcano plot depicting the gene-level differential transcriptional status for genes following degradation of IRF2BP2 for 24 hours in MV4-11. The 230 genes (out of a total of 361 genes with increased expression) that are increased in expression and bound by IRF2BP2 are depicted as red dots. All other genes bound by IRF2BP2 but not increased in expression are depicted in black. Genes not bound by IRF2BP2 are shown in grey. Differential significance was assessed using DESeq2 apeglm for shrunken fold change, |fold change expression| ≥1.5, adjusted p-value ≤ 0.1. Shown per gene are log2(fold change expression) versus -log10(adjusted p-value+0.0001).

G, Venn diagram showing the overlap between genes bound by IRF2BP2 and genes with increase in expression following treatment with dTAG-13 for 24 hours in MV4-11 cells. Two-tailed Fisher exact test was applied to test statistical significance, **** $p < 0.0001$.

H, Venn diagram showing the overlap between IRF2BP2 bound genes and increased expression following treatment with dTAG-13 for 6 (left) and 24 hours (right) in MV4-11 cells. Two-tailed Fisher exact test was applied to test statistical significance, **** $p < 0.0001$.

I, Upper panel: GSEA plots showing enrichment of signatures from IRF2BP2 bound differentially expressed genes following degradation of IRF2BP2 in MV4-11 cells. Shown

on the left is a signature derived for 24-hour treatment with dTAG-13 and assessed for enrichment in the 6-hour dTAG-13 treatment RNA-seq data. Shown on the right is a signature derived for 6-hour treatment with dTAG-13 and assessed for enrichment in the 24-hour dTAG-13 treatment RNA-seq data (GSEA significance cut-offs: |NES|≥ 1.3, p-value ≤ 0.10, FDR ≤ 0.25).

Lower panel: GSEA plots showing enrichment of the HALLMARK_TNFA_SIGNALING_VIA_NFKB within the RNA-seq data following degradation of IRF2BP2 after 6 hours (left) and 24 hours (right) (|NES|≥1, p-value ≤ 0.10, FDR ≤ 0.25).

J, Bubble plot depicting the significant enrichments in MSigDB v7.1 collection of 50 hallmark pathways within the 41 genes with increased expression after IRF2BP2 degradation for 6 hours and increased H3K27ac binding following IRF2BP2 degradation for 24 hours. Enriched gene sets are clustered in functional categories indicated by the color code; red indicates immune response signatures. The bubble size indicates the number of overlapping genes. Hypergeometric test, p ≤ 0.05, FDR ≤ 0.05.